Automated Detection and Segmentation of Vascular Structures of Skin Lesions Seen in Dermoscopy, with an application to Basal Cell Carcinoma Classification

Hagar Maher

7th, October 2018

1 Abstract

- Segmentation Approach: Given a dermoscopy image, they segment vascular structures of the lesion by first decomposing the image using independent component analysis into melanin and hemoglobin components. This eliminates the effect of pigmentation on the visibility of blood vessels. Using k-means clustering, the hemoglobin component is then clustered into normal, pigmented and erythema regions. Shape filters are then applied to the erythema cluster at different scales. A vessel mask is generated as a result of global thresholding.

- Segmentation Accuracy: The segmentation sensitivity and specificity of 90% and 86% were achieved on a set of 500000 manually segmented pixels provided by an expert.

- Classification Approach: They defined and extracted vascular features towards lesion diagnosis in Basal cell carcinoma (BCC). Among a data set of 659 lesions (299 BCC and 360 non-BCC), a set of 12 vascular features are extracted from the final vessel images of the lesions and fed into a random forest classifier.

- Classification Accuracy: When compared with a few other state-of-art methods, theproposed method achieves the best performance of 96.5% in terms of AUC in differentiating BCC from benign lesions using only the extracted vascular features.

2 Introduction

- The clinical appearance and visual properties of blood vessels in skin lesions can provide important clues for diagnosis
- The presence of vascular structures in skin lesions, their morphology and architectural arrangement could serve as a biomarker for specific conditions, especially in malignant tumors.
- Blood vessels are considered a dominant diagnostic feature in several non-melanocytic cancerous and benign skin lesions.
- Many non-cancer skin disorders are comprised of and related to vascular disorders and vasculature malformations.
- Vascular formation and angiogenesis could be an indicator of tumor development and growth.
- Detection, recognition and quantification of cutaneous blood vessels provide critical information during the evaluation of skin lesions.
- blood vessel segmentation has been a critical step towards diagnosis of retinal diseases.
- A dermoscope is a simplified microscope comprising of a high quality lens for 10 to 30-times magnification and a lighting system.
- There are major differences between the vessel segmentation problem in dermoscopic and retinal images. Retinal vessels are usually larger and hence more detectable than cutaneous vessels. Moreover, in retinal vessel analysis, the anatomy of the retina and distribution of the vessels over the image could be used as a priori information towards the segmentation problem, whereas in skin, the appearance, shape and distribution of both the lesion and blood vessels vary from image to image.
- The presence of skin pigmentation occludes the vessel visibility and further adds to the problem challenges. Therefore, specific algorithms for automatic skin vasculature analysis are still needed by addressing these problem-specific challenges.
- Cheng et al Approach: They have used a color drop algorithm in an adaptive critic design framework. They have reported the performance of their technique in terms of basal cell carcinoma (BCC) classification using vascular features. Using an artificial neural network, the classification method has achieved an area under the receiving operating characteristic of 85%. It is worth emphasizing that, although the above few methodologies are clinically meaningful, they do not specifically address the vascular segmentation problem, do not report the segmentation results quantitatively and hence do not provide quantification and morphological information of skin vasculature.

- Although dermoscopy was primarily used to study the pigmentation pattern within skin lesions, in the last decade it has been increasingly used to assess the vascular components as well.
- A number of observations on the clinical and frequency of appearance of a variety of cutaneous vascular types have been reported.
- Although these studies all confirm the importance and significant diagnostic value of cutaneous vasculature, there have been very few studies on quantitative and systematic analysis of skin vascular structures in dermoscopic images.
- There is no objective way to quantify and assess the vasculature in skin lesions.
- Visual inspection, as the only current technique in clinic, suffers from subjectivity and lack of precision.
- Vascular structures are small, complex and normally occluded by other cutaneous structures such as skin pigmentation, which makes their detection even more challenging.
- There are very few studies related to the automated analysis of cutaneous vasculature. Majority of the previous studies focus on detecting erythema rather than detecting vasculature.
- There is a great need for a framework dedicated to automatic segmentation and quantification of blood vessels in both pigmented and non-pigmented skin lesions.
- The main aim of our current investigation is to fill this gap.
- A novel framework is presented to address the detection and segmentation of cutaneous vascular structures in dermoscopy images.
- The presented method is the first attempt to develop an automatic skin vessel segmentation framework
- The proposed method incorporates skin color decomposition along with shape filtering and thus accounts for both underlying color components of the skin and the vascular shape. This eliminates the problem of vessel occlusion and further expands the applicability of the method from erythema detection to vessel segmentation.
- More accurate segmentation allows us to extract more accurate and meaningful vascular features improving the classification accuracy in differentiating BCC from non-BCC lesions.

3 Method

3.1 Overview

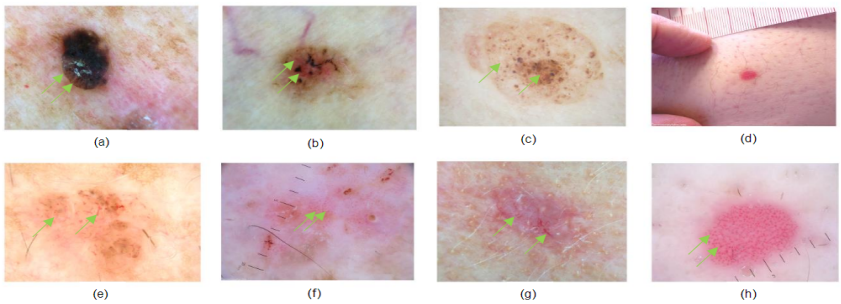

Fig. 1. Dermoscopy of a number of skin lesions with vasculature. The arrows show some of the vascular structures. (a)-(c) and (e): Presence of various morphologies of vasculature in pigmented lesions. (f) and (g): erythematous lesions with the presence of dotted and linear vascular structures. (d): Clinical image and (h) dermoscopic image of an erythematous lesion with the presence of dotted blood vessels.

- Fig. 1 demonstrates the dermoscopy images of a number of skin lesions, including a variety of different vascular patterns and erythema with or without the presence of lesion pigmentation.
- As seen in Fig. 1, pigmentation occludes the visibility of blood vessels, interferes with vascular structures and is sometimes mistakenly classified as vasculature. This causes the sensitivity and specificity of segmentation methods to fail in such cases. As a solution, we propose an approach based on skin decomposition
- Why using skin color information?

  Human skin is a multi-layered structure with various components contributing to its color. Among those, melanin and hemoglobin are the most dominantly present in the epidermal and dermal layer, respectively. Melanin, produced by melanocytes, is responsible for the characteristic brown color of human skin and hemoglobin gives blood its color and its circulation within vessels results in the red and purplish color of the skin. Both these components absorb light in the visible spectrum and this triggers the motivation to use skin color information towards understanding the underlying structures. Also, the quantities of melanin and hemoglobin in human skin are mutually independent from each other. These two valid assumptions make the basis for our analytical framework as an extension to, where ICA was first proposed for facial color image analysis
- Following the previous assumptions, They decompose the skin image into melanin and hemoglobin channels, automatically detect the hemoglobin channel and further analyze it to cluster erythematous areas and segment the vasculature using shape information.

3.2 Skin Decomposition

- Independent Component Analysis (ICA) is a computational technique to separate a multivariate signal from its constructing components and was first proposed in the skin analysis field by Tsumura.

- ICA could be applied to skin images in order to extract each of the components. Since hemoglobin is the component responsible for blood color and in order to solve the problem of skin pigmentation occluding the appearance of blood vessels, their approach is based on the extraction of melanin and hemoglobin component of skin and further analyzing the hemoglobin channel to segment the cutaneous vasculature

3.2.1 Mathamatical Approach

- Based on the modified Beer-Lambert law, in the optical density domain, total absorbed light can be expressed as a linear combination of concentrations (densities) of the underlying substances. Therefore, if I(x,y) is the color density vector in the optical density domain defined as:

$$I_{x,y} = \left[-log r_{x,y}, -log g_{x,y}, -log b_{x,y}\right]$$

  where $r_{x,y}$, $g_{x,y}$, $b_{x,y}$ are normalized color values of the RGB color space.

- Considering the above mentioned assumptions, skin color density can be modeled as a linear combination of melanin and hemoglobin quantities:

$$I_{x,y} = c^m q^m_{x,y} + c^h q^h_{x,y} + \Delta$$

  where c^m and c^h are pure color per unit density of melanin and hemoglobin respectively; and are relative quantities of melanin and hemoglobin in each pixel (x,y); Δ is the stationary column vector caused by other skin pigments and structures.

- In the conventional notation of ICA, c^m and c^h could be considered as mixing signals, q^m and q^has the source signals and $I_{x,y}$ as the observed signal.

  To achieve the best results, principle component analysis was first applied to the three dimensional input. While preserving more than 99% of the total variance of the data, the first two principle components were chosen for the analysis.

- Subsequently, ICA was applied to the input to extract the relative quantities of melanin and hemoglobin and estimate their pure color per density vectors $C = [c^m, c^h]$.

- The etimation process maximizes the non-gaussianity in the estimated components to ensure the independency among them. If we assume that the minimum quantity of each of the two components (melanin and hemoglobin) in any pixel is zero

$$\min_{x,y}\{\tilde{C}^{-1}I_{x,y}\} - \min_{x,y}\tilde{C}^{-1}\Delta = 0$$

where C is the estimated pure color density vector

- We can then define and calculate E as:

$$E = \min_{x,y}\{\tilde{C}^{-1}I_{x,y}\}$$

- Relative quantities of melanin and hemoglobin can then be obtained using the following equation:

$$\left[q^{m}_{x,y}, q^{h}_{x,y}\right]^{t} = \tilde{C}^{-1}I_{x,y} - E$$

skin decomposition is then obtained by:

$$\acute{I}_{x,y} = \tilde{C}\left(K\left[q^{m}_{x,y}, q^{h}_{x,y}\right]^{\tau} + jE\right) + j\Delta$$

- $I_{x,y}$ is the synthetized skin color. K and j are control parameters to control the quantities and effect of stationary signal, respectively.

- By setting j = 0 and k = diag[1,0] and k = diag[0,1] respectively, the melanin and hemoglobin component of the color image is extracted.

- ICA has an ambiguity on permutation. In other words, it does not automatically determine which of the two components corresponds to each chromophore. Therefore, after decomposing the skin and extracting the two component densities, it requires the expert user to determine which component represents which chromophore. As an empirical solution, considering that hemoglobin deals with the erythema and redness of the skin, the hemoglobin channel should have a correlation with redness. Knowing that a* channel in the L*a*b* color space could show the redness of an image (larger a*, more redness), the hemoglobin component is the component with higher correlation with a* channel. We modeled this concept in terms of the following equation:

$$q^h = \arg\max_i \left(corr(q^i, a^*) \right) , \mathrm{i} \in \mathrm{m}, \mathrm{h}$$

$$corr(q^i, a*) = \frac{Cov(q^i, a^*)}{\sqrt{Var(q^i)\, Var(a^*)}}$$

3.3 Erythema Extraction

- They propose three clusters within skin: normal skin, pigmented skin and erythema.
- For each cluster, a reference value vector is learned through a set of selected pixels among our images.
- To learn the reference values for the three clusters of the skin, an expert was asked to manually outline regions of normal skin, pigmented skin and vasculature among the selected pixels for training.
- ICA was applied to the selected images and the hemoglobin channel was extracted. Subsequently, three reference vectors were calculated: mean values along with the standard deviations of R, G and B channels of the hemoglobin component of the normal skin, pigmented skin and erythema as I^n, I^p and I^e, respectively.
- Once the reference values are obtained and stored as a priori information, a thresholding framework was designed based on the Mahalanobis distance on the hemoglobin component of the skin in order to classify red regions.
- For each pixel of the image, the Mahalanobis distance from the three clusters (normal skin, pigmented skin and blood vessels) in hemoglobin component is calculated and the pixel is classified into the group with the closest distance.

$$E^i_{x,y} = \sqrt{\frac{(r_{x,y}-r_i)^2}{\sigma_{ri}} + \frac{(g_{x,y}-g_i)^2}{\sigma_{gi}} + \frac{(b_{x,y}-b_i)^2}{\sigma_{bi}}}$$

$$i \in n, p, e$$

where $E^n_{x,y}$, $E^p_{x,y}$, $E^e_{x,y}$ are the Mahalanobis distances of pixel (,) from normal skin, pigmented skin and blood vessels, respectively, and ri, gi, and bi are the RGB values of the reference clusters.

- If $E^e_{x,y}$ = min ($E^n_{x,y}$, $E^p_{x,y}$, $E^e_{x,y}$), the pixel is classified as belonging to the erythematous cluster. By performing the same analysis on every single pixel of each image, each pixel is classified into the one of the three mentioned clusters.
- As a result, a mask image is produced that segments the red areas of the skin.

3.4 Shape Filtering and Vessel Mask Extraction

- Detecting redness is an essential step towards cutaneous vessel segmentation.
- There are multiple sources such as inflammation, pressure (due to contact dermoscopy imaging) and temperature that may affect skin redness and interfere with vessels.
- They proposed to take shape information into account along with color.
- For this purpose, we consider two main shape categories including tubular and circular for cutaneous vessels.
- To measure shape properties, we use and further extend the Frangi measure at 20 different scales.

$$V(X,s) = \begin{cases} 0 & if\ \lambda_2(X,s) < 0 \\ e^{\frac{-R^2(X,s)}{2\beta^2}}\left(1 - e^{\frac{-S^2}{2c^2}}\right) & otherwise \end{cases}$$

$$R = \frac{\lambda_1(X,s)}{\lambda_2(X,s)} \quad , \quad S = \sqrt{\sum_{i=1}^{2} \lambda_i^2(X,s)} \qquad |\lambda_1| \leq |\lambda_2|$$

where R,S are measures of blobness and second order structureness; $\lambda_i(X,s)$, i = 1,2 ($|\lambda_1| \leq j\lambda_2|$) are the eigenvalues of the Hessian matrix of the image I calculated at scale s; ,c are control parameters that control the sensitivity of the filter to the measures R and S

- R attains its maximum at blob-like structures and S will be low in the background where no structure is present and eigenvalues are small.
- Presence of tubular structures increases the contrast, which in turn causes the norm to become large since at least one eigenvalue will be large.
- This function maps the image into probability-like estimates of tubularness.
- We should note that the condition of equation determines the polarity of the target (dark-on-bright vs. bright-on-dark).
- Skin vessels emerge as dark structures on brighter environment (background skin). We used this prior information, derived from clinical appearance of vessels, as a consistent condition to prevent erroneous enhancements and discard structures other than vasculature.

- Depending on the orientation of blood vessels in the underlying skin layers, some of the cutaneous blood vessels may appear as circular structures (dots).
- For a pixel to belong to a circular structure, both eigenvalues of the Hessian matrix should be in the same order of magnitude. Therefore, we modified the Frangi tubularness measure to define a circularness probability estimate

$$V(X,s) = \begin{cases} e^{\frac{-(\lambda_2-\lambda_1)}{2\beta^2}}\left(1 - e^{\frac{-S^2}{c^2}}\right) & if\ \lambda_2 > \lambda_1 > 0 \\ 0 & otherwise \end{cases}$$

- Frangi measures are applied to the extracted red areas of the lesion.
- In order to include both tubular and circular shaped vascular structures, both Frangi measures are calculated for each pixel.
- The maximum value of each of the measures (9) and (10) is calculated across the scales, for each pixel.
- For each pixel, the highest value between the two is selected. Global thresholding based on Otsu's method was applied to the resulting image to get the binary vessel mask.

3.5 BCC Classification

- The presence of telangiectasia (small dilated blood vessels near the skin surface) in the lesion has been considered as a key to BCC diagnosis.
- It is worth mentioning that although BCC is classified as a non-melanocytic skin cancer, epidermis is a pigmented layer of skin with normal amount of melanin which might interfere with vessel visibility.
- There are certain types of BCC that are pigmented.
- As an application of our vascular segmentation framework, we performed a computer-assisted disease classification to differentiate skin cancer (BCC) from benign lesions.
- For this purpose, using the vessel mask resulted from the segmentation step, a set of 12 vascular features were defined and extracted from each lesion among a dataset of BCC and non-BCC lesions.
- These features include: maximum vessel length, average vessel length, standard deviation of length, maximum vessel area, average vessel area, standard deviation of vessel area, ratio of vessel area to lesion area, maximum vessel width, average vessel width, standard deviation of vessel width, number of vessel branches and ratio of branches to lesion area.

TABLE I
VASCULAR FEATURES

Feature	Description
Max_Length	Maximum length of all vessel segments in the lesion
Mean_Length	Average length of all vessel segments in the lesion
s.d._Length	Standard deviation of length of all vessel segments in the lesion
Max_Width	Maximum width of all vessel segments in the lesion
Mean_Width	Average width of all vessel segments in the lesion
s.d._Width	Standard deviation of width of all vessel segments in the lesion
Max_Area	Maximum area of all vessel segments in the lesion
Mean_Area	Average area of all vessel segments in the lesion
Area_Ratio	Ratio of vessel area to lesion area
Num_Branch	Number of vascular branches
Branch_Ratio	Ratio of number of branches to lesion area

4 Experimental Results and Discussion

The dataset used in this paper consists of 759 images obtained from three different sources:

1. Atlas of dermoscopy by Argenziano [22] comprised of images of 768 by 512 pixels by the so-called 'wet' dermoscopy approach.
2. The University of Missouri comprised of images of 1024 x 768 pixels using 'wet' dermoscopy.
3. Vancouver Skin Care Centre comprised of images of 1930 x 1779 pixels by Dermlite smartphone dermoscope with polarized light, i.e. 'dry' dermoscopy.

The diagnosis (BCC and non-BCC) of these lesions were given along with the images.

4.1 Segmentation Results

- The method implementation was performed using MATLAB 2015a.
- To obtain the reference values for the three clusters of normal skin, pigmented skin and erythema, a total of 500000 pixels from the three clusters (172320 pixels from vasculature, 163840 from pigmented skin and 163840 from normal skin) were outlined by an expert among a set of 100 images randomly chosen from the dataset.
- Fig. 3 demonstrates the distribution of the sample points of each of the three clusters in the training set in each color channel of the hemoglobin component.

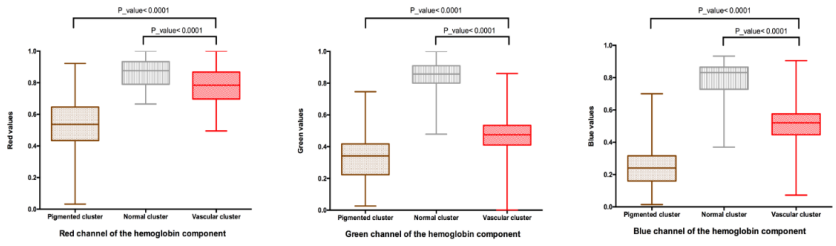

Fig. 3. RGB plane distribution of hemoglobin component among the three clusters.

- A two-sample t-test for unpaired data was performed to test the difference between the means of the three clusters.
- The results demonstrated significant difference between the mean of the erythema cluster from the other two clusters in each color channel.

- The extracted reference values (mean and standard deviation) from the training set are demonstrated in Table II.

TABLE II
GENERATED REFERENCE VALUES OF THE THREE CLUSTERS

	Pigmented	Normal	Vasculature
Red	$\mu = 0.5250$ $\sigma = 0.1385$	$\mu = 0.8625$ $\sigma = 0.0917$	$\mu = 0.7948$ $\sigma = 0.1109$
Green	$\mu = 0.3244$ $\sigma = 0.1250$	$\mu = 0.8433$ $\sigma = 0.0869$	$\mu = 0.4756$ $\sigma = 0.1108$
Blue	$\mu = 0.2390$ $\sigma = 0.0981$	$\mu = 0.7951$ $\sigma = 0.0943$	$\mu = 0.5178$ $\sigma = 0.1109$

- The remaining 659 images were used for implementation and testing.
- From the remaining image set, another set of 500000 pixels were outlined by experts (dermatologist and dermoscopist) as the ground truth for the location of vessels through manual segmentation of cutaneous vasculature regions.
- The selected test set contains both pigmented and non-pigmented lesions, different vascular patterns including tubular, curved, linear and circular vessels and different data sources (among our three dermoscopy sources).
- In the test set, among the 500k pixels, 287452 were vasculature and 212548 were chosen from non-vasculature regions. The control parameters of Frangi filter were set to $\beta = 0.7$, c = 0.05, respectively.
- FastICA implementation was used in this work by a fixed point iteration. Each lesion is decomposed into melanin and hemoglobin components.

- Fig. 4 demonstrates two BCC lesions with their associated relative hemoglobin densities.

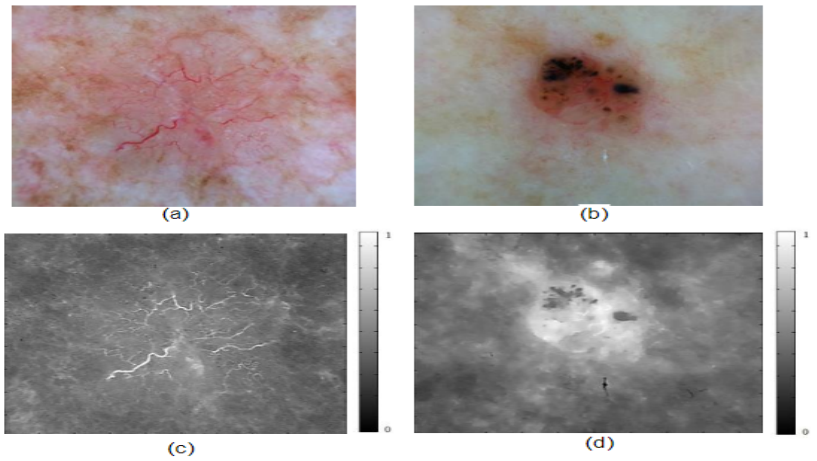

Fig. 4. Relativel hmoglobin densities of two BCC lesions.

- A number of pigmented and non-pigmented lesions along with their decomposition into melanin and hemoglobin channel are demonstrated in Fig. 5.

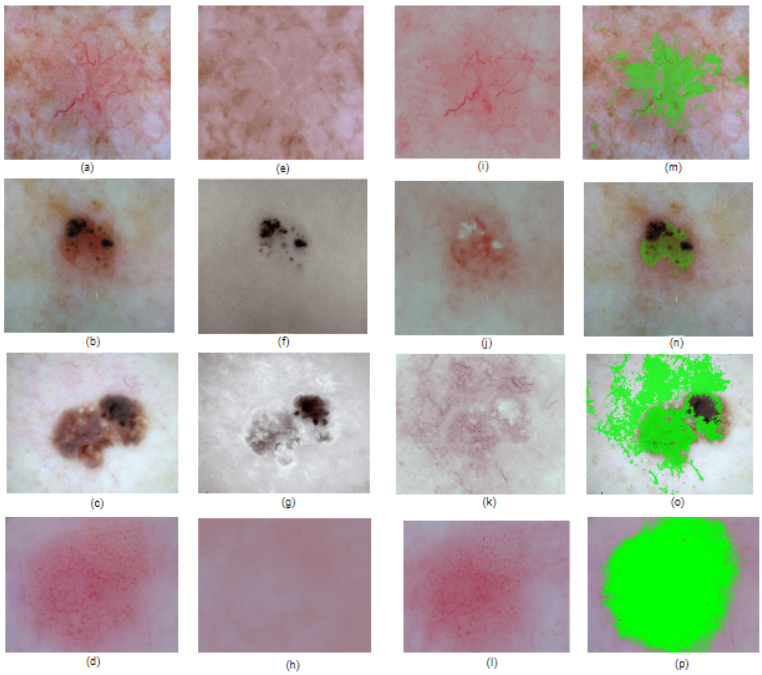

Fig. 5. ICA decomposition of lesions. (a)-(d): Original dermoscopy images of four BCC lesions. (e)-(h): Corresponding decomposed melanin channel. (i)-(l): Corresponding decomposed hemoglobin channel. (m)-(p): Segmented red areas based on the clustering of hemoglobin channel.

- They verified the performance of the empirical rule in equation (7). The component selected by this rule was compared with the one picked by the expert and among 659 images, the hemoglobin component was picked correctly 650 times (98.6% of the cases).
- The 9 cases where the hemoglobin was not correctly selected were all from contact (oil immersion) dermoscopy technique with low quality that had large areas of the image covered with bubbles which interfere with the lesion colors.
- Using the obtained reference values, k-means clustering was performed on the hemoglobin channel using the Mahalanobis distance, resulting in segmentation of red areas of the lesions as demonstrated by Fig. 5.
- The tubularness and circularness filters were applied to the extracted red regions.
- Fig. 6 shows two sample shape probability maps on the segmented red areas of lesions (a) and (b). The vessel mask is obtained as the result of Otsu's (b).

Fig. 6. Vessel shape probability maps

- The vessel mask is obtained as the result of Otsu's thresholding. Fig. 7 demonstrates the final vessel mask of the lesions, overlaid on the original image. For better visual comparison, the corresponding ground truth for the lesions are also provided.
- Segmentation performance was tested on the test set of 500000 manually outlined pixels where a sensitivity and specificity of 90% and 86% were achieved respectively.
- We would like to explain that, as mentioned in Introduction, though there have been a few related studies in the literature, vascular segmentation problem has not been addressed explicitly and hence we can't compare our segmentation results directly with other methods. Therefore, in the next section, to compare with different methods indirectly, we investigate the vessel detection and BCC classification application using different methods and different features.

4.2 Detection Results

- In order to evaluate the overall detection performance of the proposed method in terms of absence or presence of vascular patterns within the whole lesion, a detection analysis was performed.
- The proposed method was implemented on the entire 659 images, with 451 lesions containing vascular structures (Present) and 208 lesions without vascular structures (Absent).
- For each image, the number of vascular pixels detected by the proposed method and the size of the lesion (in terms of pixels) were recorded.
- To classify images into Absent or Present in terms of vascular patterns, a vascular density ratio was defined in a similar way as

$$Vascular\ Density = \frac{Vascular\ Area}{LesionSize}$$

where LesionSize is the size of lesion in terms of pixels.

- Images containing a density ratio higher than a threshold (set to 0.08) are classified as Present and the rest as Absent.
- The detection results are summarized in Table III. The performance is compared with the method proposed in, where a color-based approach using the frequency histograms of vessels in the HSL color space is used for vasculature detection.
- As it can be seen from Table III, the decomposition framework and including shape filters by our proposed method demonstrates an improved detection performance

TABLE III.
VASCULAR DETECTION PERFORMANCE

	TP Rate	FP Rate	Precision	AUC
Betta et al [12]	0.889	0.144	0.930	0.878
Proposed Method	0.933	0.100	0.952	0.922

4.3 Classification Results

- The remaining 659 images consist of 299 BCC vs 360 non-BCC lesions.
- They were processed with the steps mentioned previously (ICA decomposition, K-means clustering, redness mask extraction, shape filtering, and vessel mask extraction).
- Twelve vascular features were extracted from the extracted vessel mask images and fed into four different classifiers: simple logistic, Naïve Bayes, MLP and random forest.
- The same 10-fold cross validation was performed for each of the four classifiers and random forest yielded the best performance.
- Therefore, classification was performed using a random forest classifier composed of 100 trees, each constructed while considering 4 random features with 10-fold cross validation.
- The statistics of classification is demonstrated in Table IV. The overall weighted sensitivity and specificity for detecting BCC and non-BCC were 90.4% and 89.3%, respectively.
- The overall accuracy in term of AUC was 96.5%. As for the computational cost, the segmentation, feature extraction and classification were performed in less than 10 seconds, using a regular PC.

TABLE IV
BCC CLASSIFICATION PERFORMANCE OF THE PROPOSED METHOD

	TP Rate	FP Rate	Precision	AUC
BCC	0.859	0.061	0.914	0.965
Non-BCC	0.939	0.141	0.898	0.965
Weighted Average	0.904	0.107	0.905	0.965

4.4 Discussion

- In this study, skin decomposition was used in combination with shape analysis for vascular segmentation in dermoscopy.
- Many previous studies on different dermoscopic structures such as pigment networks, blue white veils, streaks, globules, etc. set their endpoint goal on either structure detection or disease classification rather than on the structure segmentation.
- In the case of cutaneous vasculature, there is significant clinical importance in the shape, clinical appearance and also quantification of vascular structures and hence, structure segmentation would provide useful clinical information and is a meaningful endpoint.
- Since none of the previous studies address this endpoint, in order to evaluate and compare the performance of their method, BCC classification was performed in different scenarios. Each scenario investigates the efficacy and performance of an aspect of the proposed method and is designed to evaluate the method design.
- In order to evaluate the role and necessity of shape information in our design, in this scenario shape information is ignored and only color information is used to segment the vessels.
- As such, the erythema mask resulting from the clustering of the hemoglobin channel is considered as the vessel mask.
- Similarly, in order to evaluate the importance of color information in the segmentation process, only shape information was taken into consideration, i.e. Frangi filters were directly applied to the original lesion image and thresholded to extract blood vessels.
- The same twelve vascular features were extracted in each case for classification.
- Table V compares the classification results using only vessel color or only shape segmentation by the same Random Forest classifier.

TABLE V.
BCC CLASSIFICATION PERFORMANCE USING ONLY ERYTHEMA OR SHAPE INFORMATION

	TP Rate	FP Rate	Precision	AUC
Erythema Method	0.631	0.382	0.629	0.667
Shape Method	0.712	0.312	0.712	0.791

- As it can be seen from Tables IV and V, combining both color and shape information as presented in this paper, results in better classification performance.
- The overall AUC accuracy improved from 66.7% (color only) and 79.1% (shape only) to 96.5% (combining color and shape).
- Fig. 8 shows the ROC curves of the three cases where the presented method outperforms the other two.
- It should be noted that in this work, in order to demonstrate the efficiency of our vessel segmentation method, they have only considered the vascular features of the lesion for classification.
- No preprocessing was performed on the lesions in tbeir study.
- In general, in order to provide a comprehensive diagnosis, a variety of feature categories are taken into consideration among which are patient personal profile, lesion location, lesion textural, structural and geometrical features.

- Table VI gives a comparison of our results with previous work on BCC classification in dermoscopy where different feature categories and classifiers were used. As it can be seen from Table VI, the proposed method is capable of achieving comparable or superior results compared to previous methods on a larger dataset, with less number of features and using only vascular information. The obtained vascular features could be combined with other lesion information towards a more accurate diagnosis.

TABLE VI.
COMPARISON WITH PREVIOUS WORK

	Dataset (BCC vs. Non-BCC)	# of Features	Feature Categories	Classifier	AUC
Shimizu et al. [24]	69 vs 692	25	Color, Texture, Sub-region	Layered Model	0.896
Cheng et al. [25]	350 vs 350	17	Patient profile, General & specific lesion features, General exam descriptors	EANN with GA	0.948
Cheng et al. [8]	59 vs 152	30	Vascular	Neural Net	0.955
Proposed Method	299vs 360	12	Vascular	Random Forest	0.965

4.5 Limitations

- Since the proposed method is based on the assumption that variations of skin color are mainly due to melanin and hemoglobin, the presence of artifacts that interfere with the visibility of true colors of the skin can affect the accuracy of the method.
- Fig. 9 demonstrates the dermoscopy of two lesions, where bubbles resulting from gel application, cover parts of the image.

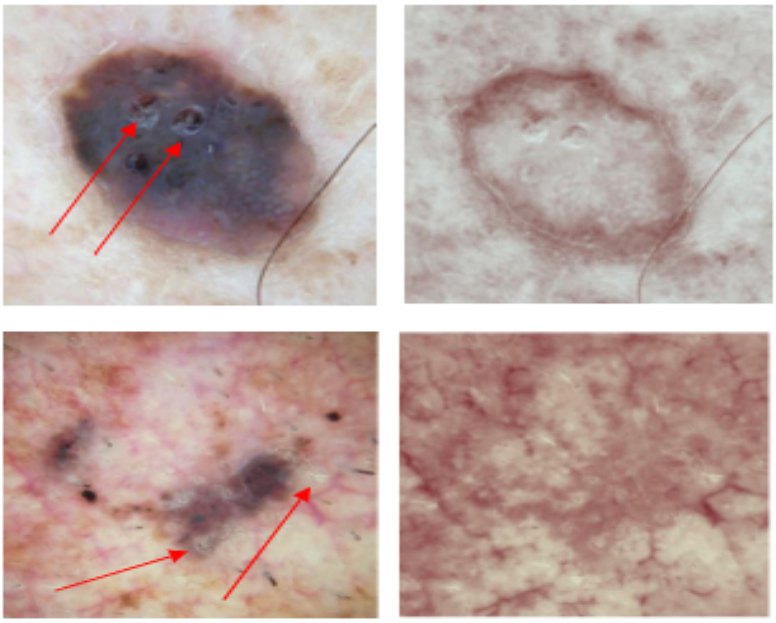

Fig. 9. Erroneous hemoglobin extraction due to the presence of bubbles. Left: Original dermoscopy of two lesion. Right: Extracted hemoglobin component. The hemoglobin component is not accurately extracted.

- As it can be seen, the presence of bubbles results in erroneous decomposition and decreases the accuracy of the extracted hemoglobin component.
- Furthermore, in this study they only consider three clusters whereas in general up to six colors may be present in skin lesions.
- Although the proposed method has demonstrated superior performance compared to previous techniques, considering more color clusters may improve the clustering accuracy.

5 Conclusion

- A fully automatic blood vessel segmentation method in dermoscopy is presented and its application in BCC classification is investigated.
- The presented method is the first in the field capable of detecting and segmenting vessels in both pigmented and non-pigmented lesions as a result of the decomposition framework.
- Compared to previous studies, this study accounts for both shape and color information and demonstrates that combining the two yields better results when segmenting cutaneous telangiectasia.
- Experimental results show the efficiency of the proposed method in extracting powerful vascular features towards BCC classification.
- The results of this study shows the promise for a potential tool for vasculature quantification which can be applied in a broad range of dermatology applications.

6 Acknowledgment

- This work was supported in part by the Canadian Institute of Health Research Grant in Skin Research and Training and Natural Sciences and Engineering Research Council of Canada.

7 Summary

7.1 Motivation

Although dermoscopy was primarily used to study the pigmentation pattern within skin lesions, in the last decade it has been increasingly used to assess the vascular components as well. Since then, there has been a number of clinical studies on the morphology and patterns of vascular structures of skin lesions where dermoscopy was used as the screening tool. So far, a number of observations on the clinical and frequency of appearance of a variety of cutaneous vascular types have been reported. Although these studies all confirm the importance and significant diagnostic value of cutaneous vasculature, there have been very few studies on quantitative and systematic analysis of skin vascular structures in dermoscopic images. There is no objective way to quantify and assess the vasculature in skin lesions. Visual inspection, as the only current technique in clinic, suffers from subjectivity and lack of precision. Moreover, vascular structures are small, complex and normally occluded by other cutaneous structures such as skin pigmentation, which makes their detection even more challenging. There are very few studies related to the automated analysis of cutaneous vasculature. Majority of the previous studies focus on detecting erythema rather than detecting vasculature. To our knowledge, there is a great need for a framework dedicated to automatic segmentation and quantification of blood vessels in both pigmented and non-pigmented skin lesions. The main aim of our current investigation is to fill this gap.

7.2 Dataset

The dataset used in this paper consists of 759 images obtained from three different sources:

1. Atlas of dermoscopy by Argenziano [22] comprised of images of 768 by 512 pixels by the so-called 'wet' dermoscopy approach.

2. The University of Missouri comprised of images of 1024 x 768 pixels using 'wet' dermoscopy.

3. Vancouver Skin Care Centre comprised of images of 1930 x 1779 pixels by Dermlite smartphone dermoscope with polarized light, i.e. 'dry' dermoscopy.

The diagnosis (BCC and non-BCC) of these lesions were given along with the images.

7.3 Framework

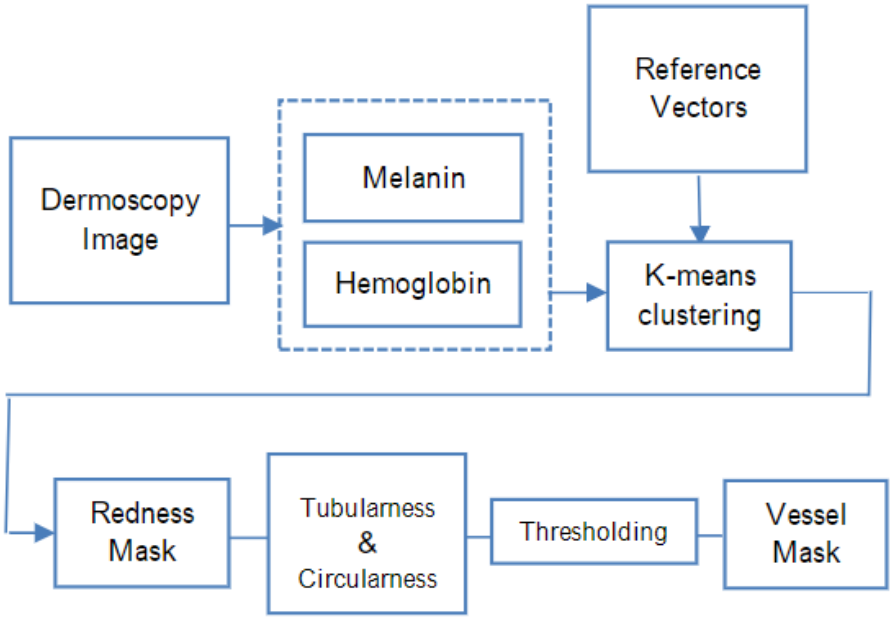

Fig. 2. Framework of the approach

A novel framework is presented to address the detection and segmentation of cutaneous vascular structures in dermoscopy images. To the best of our knowledge, the presented method is the first attempt to develop an automatic skin vessel segmentation framework. The proposed method incorporates skin color decomposition along with shape filtering and thus accounts for both underlying color components of the skin and the vascular shape. This eliminates the problem of vessel occlusion and further expands the applicability of the method from erythema detection to vessel segmentation. Furthermore, more accurate segmentation allows us to extract more accurate and meaningful vascular features improving the classification accuracy in differentiating BCC from non-BCC lesions. No preprocessing was performed on the lesions in tbeir study.

7.4 Challenge

7.4.1 Solved Challenges

1. pigmentation occludes the visibility of blood vessels, interferes with vascular structures and is sometimes mistakenly classified as vasculature. This causes the sensitivity and specificity of segmentation methods to fail in such cases. As a solution, we propose an approach based on skin decomposition.

2. ICA has an ambiguity on permutation. In other words, it does not automatically determine which of the two components corresponds to each chromophore. Therefore, after decomposing the skin and extracting the two component densities, it requires the expert user to determine which component represents which chromophore. As an empirical solution, considering that hemoglobin deals with the erythema and redness of the skin, the hemoglobin channel should have a correlation with redness. Knowing that a* channel in the L*a*b* color space could show the redness of an image (larger a*, more redness), the hemoglobin component is the component with higher correlation with a* channel

$$q^h = \arg\max_i \left(corr(q^i, a^*) \right) , \mathrm{i} \in \mathrm{m}, \mathrm{h}$$

$$corr(q^i, a*) = \frac{Cov(q^i, a^*)}{\sqrt{Var(q^i)\, Var(a^*)}}$$

3. Detecting redness is an essential step towards cutaneous vessel segmentation. However there are multiple sources such as inflammation, pressure (due to contact dermoscopy imaging) and temperature that may affect skin redness and interfere with vessels.Therefore they proposed to take shape information into account along with color.

4. It is worth mentioning that although BCC is classified as a non-melanocytic skin cancer, epidermis is a pigmented layer of skin with normal amount of melanin which might interfere with vessel visibility. In addition, there are certain types of BCC that are pigmented. Hence, as an application of our vascular segmentation framework, they performed a computer-assisted disease classification to differentiate skin cancer (BCC) from benign lesions. For this purpose, using the vessel mask resulted from the segmentation step, a set of 12 vascular features were defined and extracted from each lesion among a dataset of BCC and non-BCC lesions.

5. Though there have been a few related studies in the literature, vascular segmentation problem has not been addressed explicitly and hence

they can't compare their segmentation results directly with other methods. Therefore, to compare with different methods indirectly, they investigate the vessel detection and BCC classification application using different methods and different features.

7.4.2 Challenges Not Solved

Since the proposed method is based on the assumption that variations of skin color are mainly due to melanin and hemoglobin, the presence of artifacts that interfere with the visibility of true colors of the skin can affect the accuracy of the method.

Furthermore, in this study they only consider three clusters whereas in general up to six colors may be present in skin lesions.

Although the proposed method has demonstrated superior performance compared to previous techniques, considering more color clusters may improve the clustering accuracy.

7.5 Results

- Segmentation performance was tested on the test set of 500000 manually outlined pixels where a sensitivity and specificity of 90% and 86% were achieved respectively.
- As it can be seen from Table III, the decomposition framework and including shape filters by our proposed method demonstrates an improved detection performance

TABLE III.
VASCULAR DETECTION PERFORMANCE

	TP Rate	FP Rate	Precision	AUC
Betta et al [12]	0.889	0.144	0.930	0.878
Proposed Method	0.933	0.100	0.952	0.922

- The overall accuracy in term of AUC was 96.5%. As for the computational cost, the segmentation, feature extraction and classification were performed in less than 10 seconds, using a regular PC.

TABLE IV
BCC CLASSIFICATION PERFORMANCE OF THE PROPOSED METHOD

	TP Rate	FP Rate	Precision	AUC
BCC	0.859	0.061	0.914	0.965
Non-BCC	0.939	0.141	0.898	0.965
Weighted Average	0.904	0.107	0.905	0.965